JOURNAL OF ENVIRONMENTAL SCIENCES 40 (2016) 161–168

Available online at www.sciencedirect.com

ScienceDirect

www.elsevier.com/locate/jes

JES JOURNAL OF ENVIRONMENTAL SCIENCES

www.jesc.ac.cn

Size and elemental composition of dry-deposited particles during a severe dust storm at a coastal site of Eastern China

Hongya Niu[1,2], *Daizhou Zhang*[3], *Wei Hu*[1,3], *Jinhui Shi*[4], *Ruipeng Li*[4], *Huiwang Gao*[4], *Wei Pian*[2], *Min Hu*[1,*]

1. *State Key Joint Laboratory of Environmental Simulation and Pollution Control, College of Environmental Sciences and Engineering, Peking University, Beijing 100871, China*
2. *Hebei Collaborative Innovation Center of Coal Exploitation, Hebei University of Engineering, Handan 056038, Hebei, China*
3. *Faculty of Environmental and Symbiotic Sciences, Prefectural University of Kumamoto, Kumamoto 862-8502, Japan*
4. *Key Laboratory of Marine Environmental Science and Ecology, Ocean University of China, Ministry of Education, Qingdao 266100, China*

ARTICLE INFO

Article history:
Received 15 May 2015
Revised 27 August 2015
Accepted 14 September 2015
Available online 11 January 2016

Keywords:
Asian dust
Dry deposition
Morphology
Size distribution
Elemental composition

ABSTRACT

Dry-deposited particles were collected during the passage of an extremely strong dust storm in March, 2010 at a coastal site in Qingdao (36.15°N, 120.49°E), a city located in Eastern China. The size, morphology, and elemental composition of the particles were quantified with a scanning electron microscope equipped with an energy dispersive X-ray instrument (SEM–EDX). The particles appeared in various shapes, and their size mainly varied from 0.4 to 10 μm, with the mean diameters of 0.5, 1.5, and 1.0 μm before, during, and after the dust storm, respectively. The critical size of the mineral particles settling on the surface in the current case was about 0.3–0.4 μm before the dust storm and about 0.5–0.7 μm during the dust storm. Particles that appeared in high concentration but were smaller than the critical size deposited onto the surface at a small number flux. The elements Al, Si and Mg were frequently detected in all samples, indicating the dominance of mineral particles. The frequency of Al in particles collected before the dust storm was significantly lower than for those collected during and after the dust storm. The frequencies of Cl and Fe did not show obvious changes, while those of S, K and Ca decreased after the dust arrival. These results indicate that the dust particles deposited onto the surface were less influenced by anthropogenic pollutants in terms of particle number.

Introduction

Dust particles play an important role in the earth's environmental evolution and conservation (Chadwick et al., 1999; Neff et al., 2008). Asian dust, which comes from the arid and semi-arid areas of northwestern China and Mongolia, spreads from the Asian continent to the northern Pacific and even to North America (Duce et al., 1980; VanCuren and Cahill, 2002). Evidence has confirmed that the dust input to the ocean fertilizes the growth of phytoplankton in the surface of sea water (Calil et al., 2011; Shi et al., 2012), and that the dust input to islands prevents the ecological degradation caused by soil erosion (Kennedy et al., 1998; Simonson, 1995). The long-distance transport and settlement of dust particles also provide nutrients to rainforest and soil formation worldwide (Swap et al., 1992; Tiessen et al., 1991). Understanding the physical and chemical properties of deposited dust particles would be greatly beneficial to the

* *Corresponding author*. E-mail: minhu@pku.edu.cn (Min Hu).

http://dx.doi.org/10.1016/j.jes.2015.09.016

quantitative evaluation of their effects on and roles in the evolution and conservation of the ecosystem.

The process whereby particles settle to the surface is governed by particle deposition velocity. The dry deposition velocity of a particle is usually estimated based on particle size and density, in consideration of the resistance of the air and surface (Lin et al., 1994; Qi et al., 2006; Zhang et al., 2004). Therefore, the dust flux to the surface significantly depends on the number size distribution, mass concentration, and settling velocities of the particles. In some studies, the sediments in the deep-sea or on the Loess Plateau were evaluated by estimating the sedimentation of different geologic ages and the relation between sedimentation and Paleoclimate (Ding et al., 2001; Olivarez et al., 1991; Soreghan, 1992). The dry deposition flux of the suspended particles in numerical models was directly derived by multiplying the measured dust mass concentration with theoretically calculated dry deposition velocity. The majority of these studies did not consider the wide range of particle size or the meteorological conditions (Lawrence and Neff, 2009; Li et al., 2011).

Dry-deposited particles have rarely been directly measured and data on their morphology, size, and chemical compositions are very limited. Moreover, limited information is known about the morphology, size, and chemical composition of dry-deposited particles, and the dust deposition flux to the surface has not been well validated based on field measurements. Long-term sampling is required to obtain a measureable amount of particles because of the slow process of dry deposition (Graydon et al., 2008; Shahin et al., 2000). For instance, at least two-day samples were required for the dust deposition (Hsu et al., 2010) and more than 1 week for the dry deposition fluxes and the mass size distributions of different species (Paode et al., 1998). The problem in sampling long-term deposited particles is that short-term-deposited dust storm particles are difficult to separate from the particles deposited during the non-dust time. Therefore, dust storm samples collected over periods of several hours are necessary to accurately describe the evolution and dry deposition of particles. Moreover, the overlap of particles on a filter must be avoided to obtain the exact characteristics of the target particles. Electron microscopy analysis is an approach for characterizing the morphology and composition of particles individually. This approach accurately describes the dust particles deposited onto the surface and demonstrates dust deposition with dust passage.

In this study, dry-deposited mineral particles were collected during passage of a dust storm in Qingdao, a coastal city in China. The mineral particles deposited onto the surface were identified and investigated in terms of their morphology and elemental composition, which were obtained with a scanning electron microscope equipped with an energy dispersive X-ray instrument (SEM–EDX). The characteristics of the dry-deposited particles were compared with those of suspended dust particles previously recorded at the same site. The purpose was to specify the similarities and differences of these particles to better understand the deposition process of dust particles after long-range transport. The evolution of dry-deposited dust particles during the dust storm passage was described according to the characteristics of the particles collected in different stages.

1. Methods

The particles deposited onto the surface were collected on the roof of a building at the campus of Ocean University of China in Qingdao (36.15°N, 120.49°E) between the 16th and 24th of March, 2010, during which a dust-loaded cyclone passed through the city. The details of the sampling periods and weather conditions are listed in Table 1. The dust storm was caused by a cyclone in western and south-central Mongolia, according to satellite observations, and then was transported to Beijing by the cyclone under a strong (>10 m/sec) north-west wind (Chen et al., 2012; Wang et al., 2014). The dust loaded in the low pressure system was an extreme dust storm according to the daily mean total suspended particulates (TSP, 3400 $\mu g/m^3$) and PM_{10} (1500 to 3500 $\mu g/m^3$) measured in Beijing (Chen et al., 2012). This dust storm was an extremely strong one in its dispersion and extent of influence. The deposition and dust loading were all greater than in previous years (Hsu et al., 2013; Li et al., 2011).

The samples were passively collected onto electron microscopic Ti grids with the use of a collection cask (approximately 25 cm high). The grids were fixed on a stainless cylinder (with a height of 1 cm high and a diameter of 12 cm), which was set on the bottom of the cask. The collection time for each sample was between 12 and 31 hr, which was determined according to the status of air pollution. After collection, the grids were separately conserved in small capsules, which were sealed in a plastic bag with silica and were reserved in a refrigerator until subsequent analysis. Consequently, samples on ten Ti grids were obtained, two Ti grids for each sample. One Ti grid in each sample was analyzed in this study, and the other one was kept for further analysis. Accordingly, the results of this investigation were based on five Ti sample grids.

The particles on the grids were investigated and imaged with SEM to identify their morphology and size. About 40 images of the particles on each grid were randomly taken. The equivalent diameter of a particle, which was defined as the diameter of a circle that had the same projection area as the measured particle in the electron microscope image, was used as the particle size. Hereafter, "equivalent diameter" is expressed as "geometric size". The elemental composition of the particles in a few images was determined with the EDX spectrometer attached to the SEM. After the image was taken, every particle in the image was analyzed. The SEM was

Table 1 – Sample collection and weather condition.

Sample ID	Start (BST)	End	Weather condition
QD01	08:40 March, 16th	20:45 March, 16th	Floating dust
QD02	08:57 March, 19th	21:40 March, 19th	Blowing dust
QD03	21:50 March, 19th	21:56 March, 20th	Dust storm
QD04	22:08 March, 20th	18:40 March, 21st	Blowing dust
QD05	09:00 March, 23rd	15:45 March, 24th	Floating dust

BST: Beijing standard time (8 hr prior to GMT). QD01, QD02, QD03, QD04, and QD05 refer to samples collected in normal polluted urban atmosphere, the polluted urban atmosphere before and during the dust storm, and after the dust storm. GMT: Greenwich mean time.

operated at 10 keV accelerating voltage. The X-ray spectrum of a particle was generated under the accelerating voltage of 20 keV and was collected for 30 sec. EDX could identify the elements of atomic number larger than 5, except nitrogen, which could only be detected in the initial seconds if present, and volatile components were not considered. The atom number and weight fractions of the elements in the particles were estimated with ZAF (Z: element atomic number; A: X-ray absorption; F: X-ray fluorescence) calibration (Zhang et al., 2003a).

An optical particle counter (Rion KR-12 A, Rion Corporation, Japan) was used to measure the size-segregated number concentrations of the particles in ambient air every 15 min during the entire period. The available diameter ranges were 0.3–0.5, 0.5–0.7, 0.7–1.0, 1.0–2.0, 2.0–5.0, and >5.0 μm.

2. Results

2.1. Passage of the dust-loading cyclone

The cold front of the dust-loaded cyclone arrived in Qingdao at about 03:00 BST (Beijing standard time, Greenwich mean time (GMT) + 8 hr) on the 20th of March, 2010 (Fig. 1). The approach of the cold front increased the temperature by 7°C, but decreased the pressure from 1011 to 990 hPa. The number concentrations for particles in the size range of 1.0–2.0 μm and 2.0–5.0 μm were shown together as the range of 1.0–5.0 μm because their variations were similar. The number concentrations of the suspended particles whose sizes ranged from 1.0 to 5.0 μm and larger than 5.0 μm dramatically increased, by one or two orders of magnitude, from 10^7 to 10^8 m^{-3} and from 10^5 to 10^7 m^{-3}, respectively. The number concentration of the suspended particles in the size range of 0.3–0.5 μm was also increased by 50%. After the cold front arrived, the temperature and relative humidity presented diurnal variations, and the pressure increased to about 1010 hPa. The number concentration of the particles ranging from 1.0 to 5.0 μm was even higher than those ranging from 0.3 to 0.5 μm. This observation indicates the extreme strength of the dust storm. After the passage of the cold front, the meteorological conditions and particulate concentrations returned to normal levels. For example, the number concentration of the particles ranging from 0.3 to 0.5 μm was about 10^8 m^{-3} after the dust storm, which was similar to that before the storm. Based on the sampling record, weather conditions, and air pollution level, QD01 was a sample collected in the normal polluted urban atmosphere, QD02 was a sample collected in the polluted urban atmosphere just before the dust storm arrival, the QD03 sample was collected during the dust storm, and the QD04 and QD05 samples were collected after the dust storm.

2.2. Particle category according to morphology and elemental composition

The particles deposited onto the Ti grids and the EDX spectra of a few particles are illustrated in Fig. 2. Ti in EDX spectra is caused by the grid. The particles shown in Fig. 2a, b, c, and d were from samples QD01, QD02, QD03, and QD05, respectively. Based on their morphologies and elemental compositions,

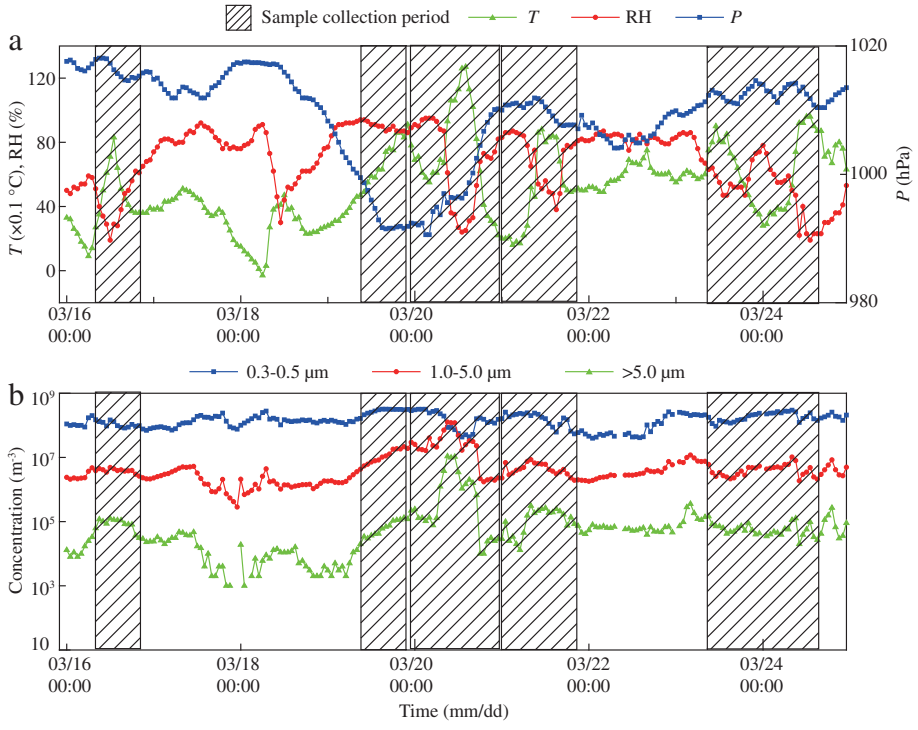

Fig. 1 – Time series of meteorological conditions including the temperature (*T*), relative humidity (RH), pressure (*P*), and the number concentrations of particles recorded by the optical particle counter in different size ranges. Beijing standard time (GMT + 8 hr) is used in this figure. GMT: Greenwich mean time.

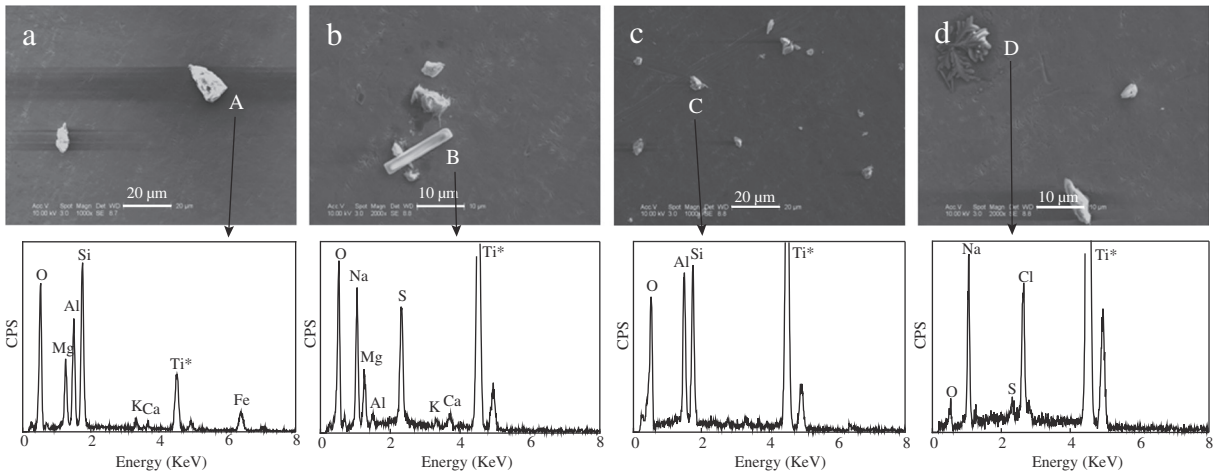

Fig. 2 – SEM pictures and EDX spectra of particles (a) A, (b) B, (c) C, and (d) D collected in the dust storm. SEM: scanning electron microscopy; EDX: energy dispersive X-ray spectrometer; CPS: X-ray counts.

the particles were categorized into three groups (Table 2), namely, aluminum–silicon (Al–Si) mineral particles, sodium–sulfur (Na–S) mineral particles, and aged sea salt particles. The Al–Si mineral particles were irregularly shaped, and they did not change or exhibit volatility under the electron beam. These particles mainly consisted of Al and Si with/without other mineral elements (particles A and C in Fig. 2). The Na–S mineral particles had a narrow-long shape, were stable under the electron beam, and were generally composed of Na, S, and Mg with minor prevalence of Al, K and Ca (particle B in Fig. 2). The appearance of aged sea salt particles was comparable to the tissue of leaves, and they were abundant in Na and Cl with insignificant existence of S or Mg (particle D in Fig. 2). A few particles could not be categorized into the groups specified above because of their exceedingly small number and were therefore excluded in the subsequent description and discussion.

Given that sample QD01 was collected before the dust storm, the mineral particles were considered to mainly be from local and regional sources, such as surface soil dust and road dust, but not from the desert areas in northwest China. Sample QD02 had the largest number fraction of aged sea salt particles and smallest number fraction of Al–Si mineral particles. Na–S and Al–Si mineral particles occupied a large fraction in QD02. These particles were those that could be observed in polluted urban atmosphere and were not dust particles from desert areas, and may have originated from anthropogenic activities. In contrast, the Al–Si and Na–S mineral particles in the QD03 sample were considered to be dust particles from desert areas. Meanwhile, the mineral particles in the QD04 and QD05 samples included mineral particles from desert areas, and from local and regional areas also. These particles were relatively similar to those in the QD01 sample.

Table 2 – Number fractions (%) of different type particles according to elemental composition.

Sample ID	Al–Si mineral particle	Na–S mineral particle	Aged sea salt
QD01 (57)	66.7	14.0	8.8
QD02 (94)	43.7	13.8	25.5
QD03 (127)	65.3	18.9	0.8
QD04 + QD05 (106)	52.9	27.4	7.5

The total numbers of detected particles with EDX (energy dispersive X-ray) spectra for different samples are listed in parentheses.

2.3. Size distribution of dry-deposited particles

The number size distribution of dry-deposited and suspended particles measured with the optical particle counter during the sampling period is depicted in Fig. 3. Geometric size, which is defined by the equivalent diameter, refers to the size of dry-deposited particles according to their projection areas on the Ti grids. The size of the suspended particles measured with the optical particle counter was estimated from the forward scattering of the particle. Sakai et al. (2008) compared the size of dust particles obtained *via* an optical particle counter with that obtained with electron microscope images. Consequently, the researchers reported that the former was 5% to 13% larger than the latter. The distributions were compared without calibration in the current study because the difference was small. These two kinds of number size distribution were compared to demonstrate the possible critical size (equal to or larger than which, the particles will rapidly deposit onto the surface) for dry-deposited particles, which is important for their flux calculation (Zhang et al., 2005a; Zhang, 2008).

The number size distribution of the deposited particles was broad, and the particles primarily ranged from 0.4 to 10 μm for the entire observation period. The mean diameter of the deposited particles was around 0.5, 1.5, and 1.0 μm before, during, and after the dust storm, respectively. Two modes in the size distribution of the QD01 sample were observed. The first mode was around 1.0 μm, and the other was around 3.0–4.0 μm. The average number size distribution recorded with the optical particle counter revealed that one mode ranged from about 2.0 to 5.0 μm. In the QD02 sample, the modes of the deposited particles were approximately 0.5 μm and 4.0–5.0 μm, while that of the suspended particles roughly varied

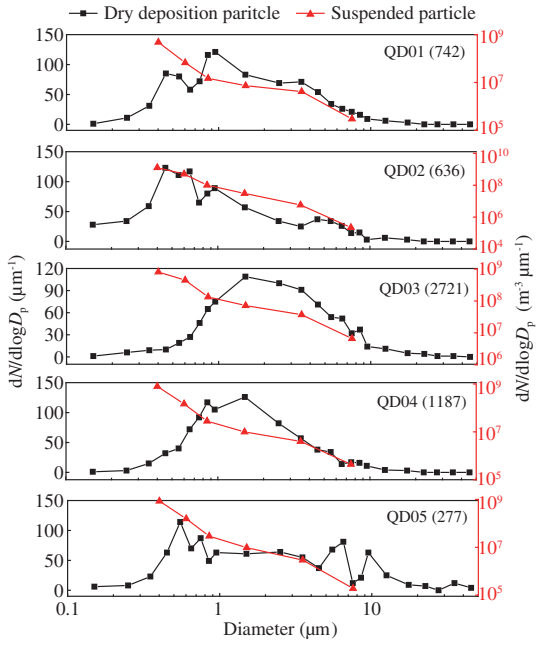

Fig. 3 – Number size distribution ($dN/dlogD_p$) of the detected dry-deposited particles and as well as suspended particles measured by the optical particle counter in different stages of the dust storm. Numbers of dry-deposited particles for different samples are listed in parentheses. *N*: particle number; D_p: particle size; QD01, QD02, QD03, QD04, and QD05 refer to Table 1.

between 2.0 to 5.0 μm. In the QD03 sample, the number size distribution of the deposited particles was close to a lognormal distribution with a mode of 1.5 μm. Meanwhile, the distribution of the suspended particles in this sample was almost linear, with a small slope. In the QD04 sample, the mode of the deposited particles was also around 1.5 μm, and it marginally shifted to smaller size. The number of the suspended particles sharply decreased, *i.e.*, from 0.3–0.5 to 0.7–1.0 μm, and from 2.0–5.0 to larger than 5.0 μm. In the QD05 sample, the distribution of the deposited particles displayed a slight zigzag pattern, with modes varying from 0.5 to 0.6 μm, and from 6.0 to 7.0 μm. The distribution of the suspended particles in this sample was similar to those in the QD01 sample.

The above findings indicate that the number size distribution of the deposited particles was influenced by the dust storm process during the sample collection. The size distribution of the particles before (QD01 and QD02) and after (QD05) the dust storm had bimodal characteristics, with fine mode around 0.3–0.7 μm and coarse mode around 3.0–7.0 μm. This showed that the polluted local urban atmosphere contained both fine and coarse mode mineral particles. The dominant elemental compositions of the particles at these two modes were Al and Si. Under the influence of the dust plume (QD03 and QD04), the distributions of the deposited particles showed single width modes, whose size ranged from 0.7 to 10.0 μm (QD03) and from 0.5 to 6.0 μm (QD04), with the peak varying between 1.0 and 2.0 μm. The dust plume brought more coarse particles into the atmosphere and blew away the fine particles.

2.4. Elemental composition of mineral particles

The number fractions of the dust particles containing different elements in the deposited mineral particles are displayed in Fig. 4, representing the relative number concentration of particles containing a particular element. Si-containing particles were considered as mineral particles. The detection frequencies of trace elements, such as Cr and Mn, were low and not included in the figure. The frequency of Cl (2% to 4%) was extremely low in all samples. The elements Mg and Al were most frequently detected in the particles during the different stages of the dust storm after Si. The frequency of Al in all samples was about 74% to 88%. This frequency decreased when the dust storm approached (QD02), whereas it increased during the dust storm (QD03). Before the dust storm (QD01), the detection frequencies of some elements, such as Mg, K, and Fe, were higher than those in other stages, particularly for Mg, with a frequency of 67%. The frequencies of S and Ca in QD01 were 26% and 39%, respectively, which were slightly lower than those obtained when the dust storm was approaching and were higher than those in other stages.

The frequencies of Na, S, and Ca increased when the dust storm approached, whereas those of Mg, Al, Cl, K, and Fe decreased. During the dust storm, the frequencies of Na and Cl were almost the same as those before the dust arrival, while those of Mg, Al, K and Fe were relatively higher. After the dust storm, the frequency of Al decreased and was similar to that before the dust storm. The frequencies of Mg, K, Ca, and Fe obviously decreased, whereas those of Na, S, and Cl slightly increased.

The comparison of the elements in particles collected during the different stages of the dust storm revealed that the air, as the dust storm approached, contained more anthropogenic polluted particles, based on the lower number frequencies of Mg and Al and the higher number frequencies of S and Ca. The dust plume had more crustal particles, shown by the lower number frequency of S and the higher number frequencies of Mg and Al. After the dust storm, the airborne mineral particles were mainly composed of crustal and local emission particles based on the higher number frequencies of Na and Al.

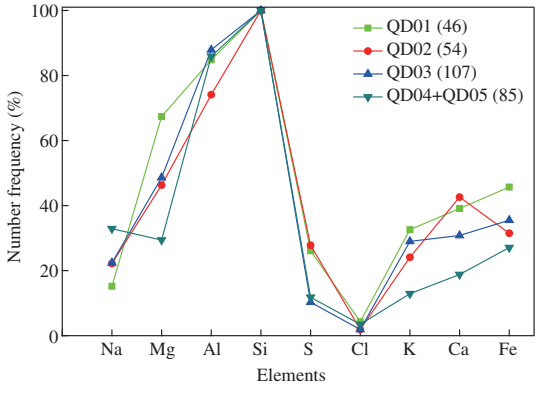

Fig. 4 – Number frequencies of particles containing different elements in detected dust particles. The numbers of detected dust particles in each sample are in parentheses.

The relative weight content of Al, S, and Ca (Fig. 5) was compared to investigate the sulfurization of the mineral particles during the dust storm. Sulfurization refers to sulfate formation on the dust particles. Such a formation was identified by the presence of S in the particles, with the assumption that all S was sulfate and produced *via* the particle surface process. The number ratios of the particles on the line of Al (the relative weight ratio of S was zero) were 70%, 43%, 81%, and 78% in the QD01, QD02, QD03, and QD04 + QD05 samples, respectively. The sulfurization ratios (the number of sulfurized particles to that of the total particles used in each triangle diagram) were high as the dust storm approached (QD02), but low during the dust storm (QD03). The distributions of the particle contents Ca and S were close to $CaSO_4$ when the dust storm approached. At the same time, the particles on the line of Ca accounted for 26% of the total mineral particles. The sulfurization ratios were 16%, 9%, 4%, and 5% for the particles inside the triangles, except those on the edges, in different stages of the dust storm. In sum, the sulfurization ratio of the mineral particles was higher when the dust storm approached, but was lower during the dust storm. The low sulfurization ratio was similar to S number fractions shown in Fig. 4.

3. Discussion

Only a few data regarding individual Asian dust particles deposited onto the surface are available. The deposited mineral particles in this study had irregular shapes. This observation is similar to those for suspended dust particles reported in previous studies (Ma et al., 2012; Shi et al., 2005). By adopting individual particle analysis, Zhang et al. (2003a) examined the number size distribution of suspended dust particles in Qingdao during dust storms. These researchers discovered that the particles generally ranged from 1.0 to 8.0 μm, with a mode of about 3.0 μm. Sheng et al. (2003) also reported that the size distribution of suspended dust particles primarily varied between 2.0 and 7.0 μm. Pan and Wang (2015) conducted dry deposition measurements at five sites, and found that the size distribution of trace elements was mainly concentrated in the range 0.2–10.0 μm, and the crustal elements (Al and Fe) had bimodal peaks at about 0.5 and 5.0 μm. Zhang et al. (2003b) observed dust storm events near the desert regions, and found that the mass mean diameter of the suspended dust particles was around 4.5 μm. Yan et al. (2012) also reported that the mode was around 3.3–4.7 μm for the suspended dust particles in Qingdao. The size distribution of the particles in the current study ranged from 0.4 to 10 μm, which was wider for the deposited particles. The mode of the deposited dust particles was around 1.5 μm, which was smaller than that of the suspended particles. After being transformed into volume-size distributions, the mode sizes in this study were close to the sizes reported in previous studies. Similar results were also confirmed for dust particles after long-distance travel in the marine atmosphere (Fukushima and Zhang, 2015).

In general, mineral particles larger than a certain size are likely to be deposited onto the surface more efficiently than smaller particles during dust storms (Zhang et al., 2005a). In this study, critical size was defined as the threshold size for dust particles to be deposited. The particles larger than the

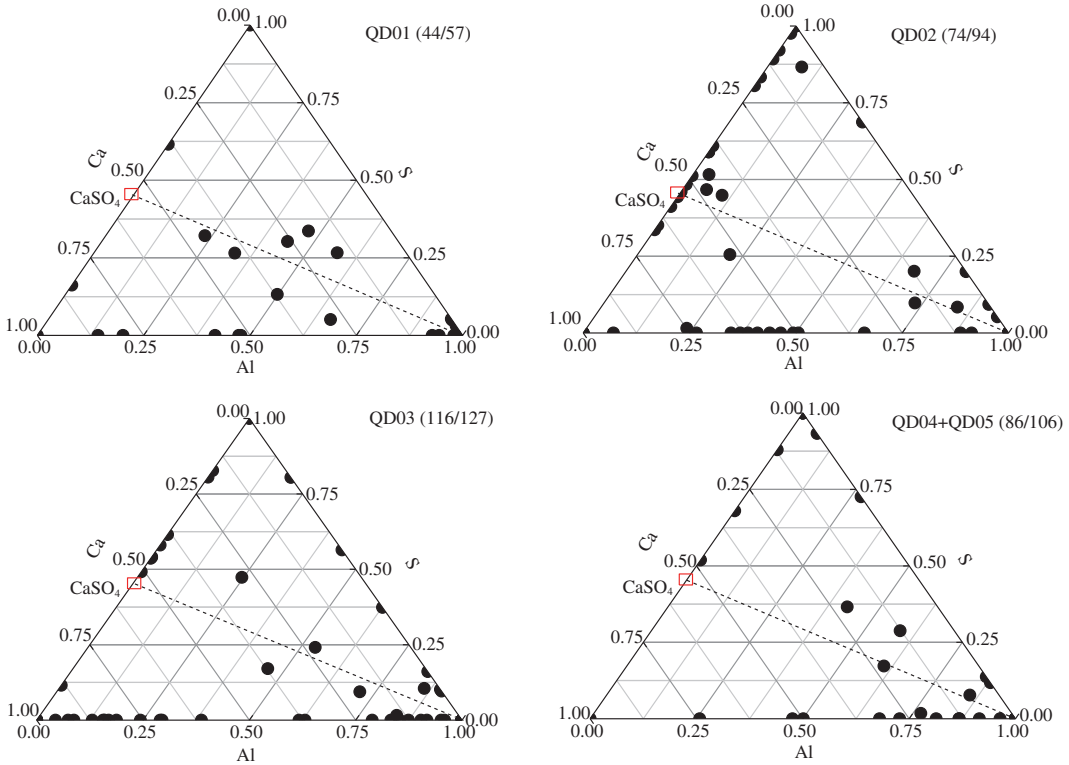

Fig. 5 – Relative weight ratios of Al, S and Ca in mineral particles. Numbers in parentheses are ratios of particles appearing in the triangle to quantitatively detected particles in each sample.

critical size are removed from the air to the surface *via* dry deposition more quickly and efficiently than smaller particles, thereby increasing the number flux of the deposited particles. By comparing the deposited and suspended particles, this study determined that the critical size of the particles before the dust storm ranged from 0.3 to 0.4 μm (Fig. 3). With the same method, the critical size of the particles during the storm was identified to vary between 0.5 and 0.7 μm, and it was around 0.55 μm after the dust storm. The critical size was in the submicron range. One reason for this circumstance may be the drag effect of fine dust particles by the coarse dust particles during the long-range transport (Wang and Xia, 2004; Zhang et al., 2008). Another probable explanation for this phenomenon may be the result of the mixture of dust particles with other particles, which substantially regulates particle settlement (Zhang, 2008). High mixture degrees make it easier for the deposited particles to settle. Smaller particles have larger surface effects, which favor their adherence to other particles.

The major elements of the dry deposition dust particles were Mg, Al, Si, and Fe, which were similar to those of suspended dust particles from different areas (Okada and Kai, 2004; Zhang and Iwasaka, 1999; Hsu et al., 2013). Zhang and Iwasaka (1999) reported that Mg, Al, Si, K, Ca, and Fe were the main elements of dust particles collected from Beijing. The frequency of Na-, S-, and Cl-containing dust particles was 22%, 10%, and 2%, respectively, during the dust storm. These elements were approximately at the same levels as those observed by Zhang et al. (2003a) in Qingdao except for Cl, which was lower in the current study. The number fraction of S was 28% as the dust storm approached in the current study. This value was higher than that of the suspended particles collected in a dust storm in Qingdao (Zhang et al., 2005b). The frequency of S was higher as the dust storm approached, indicating the efficient formation of sulfate *via* heterogeneous reactions on particles before the dust arrival, compared with those in the dust plume. The deposition of Fe in mineral aerosols was influenced by the anthropogenic emissions of S or organic acids during the atmospheric transport (Li et al., 2012; Mahowald et al., 2005; Meskhidze et al., 2003), whereas the frequency of Fe did not significantly change during the dust storm, which is different from the results by Pan and Wang (2015).

4. Summary

Dry-deposited particles collected during the different stages of an extremely strong dust storm passage at a coast site in East China in March 2010 were analyzed. The particles were identified according to their morphology, size distribution, and elemental composition. The deposited mineral particles were irregular, which was also the case for the suspended mineral particles reported in previous studies. The size of the deposited dust particles mainly ranged from 0.4 to 10 μm, with mean diameters between 0.5 and 1.5 μm before, during, and after the dust storm. In the current case, the critical size of the deposited dust particles was 0.5 to 0.7 μm, which was slightly larger than that of the mineral particles from local areas. The deposited mineral particles had a wider size distribution and smaller size mode than the suspended particles previously reported. The elements of Mg, Al, and Si dominated in all samples, indicating the dominance of mineral particles. The frequency of S was high as the dust storm approached, but it was decreased during and after the dust storm. The sulfurization of the mineral particles displayed a similar trend. The major elements of the deposited particles were similar to the characteristics of the suspended particles in previous studies. The information this study presented on the physical and chemical properties of the deposited dust particles would significantly benefit the accurate evaluation of the deposition flux of mineral components due to dust storms, although the results and conclusions are limited to this case study.

Acknowledgments

This work was supported by the National Basic Research Program of China (No. 2013CB228503), the National Natural Science Foundation of China (Nos. 91544214, 21190052, 41121004, 41541038), and the Education Bureau of Hebei Province for Excellent Young Scholars (No. YQ2014020). The design and field measurements of this study were initiated under the foundation of the JSPS Grant-in-Aid for scientific research (C). We would like to thank Nicholas James O'Connor and Dr. Anindita Dutta for their assistance in improving the language of the manuscript.

REFERENCES

Calil, P.H.R., Doney, S.C., Yuminoto, K., Eguchi, K., Takemura, T., 2011. Episodic upwelling and dust deposition as bloom triggers in low-nutrient, low-chlorophyll regions. J. Geophys. Res. Atmos. 116 (C6), C06030.

Chadwick, O.A., Derry, L.A., Vitousek, P.M., Huebert, B.J., Hedin, L.O., 1999. Changing sources of nutrients during four million years of ecosystem development. Nature 397 (6719), 491–497.

Chen, H., Zhao, L.N., Zhao, L.Q., Tian, H., Wu, H., Huan, N., 2012. Effects of sand dust weather on the air quality of Beijing. Res. Environ. Sci. 25 (6), 609–614.

Ding, Z.L., Yu, Z.W., Yang, S.L., Sun, J.M., Xiong, S.F., Liu, T.S., 2001. Coeval changes in grain size and sedimentation rate of eolian loess, the Chinese Loess Plateau. Geophys. Res. Lett. 28 (10), 2097–2100.

Duce, R.A., Unni, C.K., Ray, B.J., Prospero, J.M., Merrill, J.T., 1980. Long-range atmospheric transport of soil dust from Asia to the tropical North Pacific: temporal variability. Science 209 (4464), 1522–1524.

Fukushima, S., Zhang, D., 2015. Comparison in size and elemental composition of dust particles deposited to the surface and suspended in the air on the southwest Japan coast. Atmos. Environ. 118, 157–163.

Graydon, J.A., St. Louis, V.L., Hintelmann, H., Lindberg, S.E., Sandilands, K.A., Rudd, J.W.M., et al., 2008. Long-term wet and dry deposition of total and methyl mercury in the remote Boreal ecoregion of Canada. Environ. Sci. Technol. 42 (22), 8345–8351.

Hsu, S.C., Wong, G.T.F., Gong, G.C., Shiah, F.K., Huang, Y.T., Kao, S.J., et al., 2010. Sources, solubility, and dry deposition of aerosol trace elements over the East China Sea. Mar. Chem. 120 (1–4), 116–127.

Hsu, S.C., Tsai, F., Lin, F.J., Chen, W.N., Shian, F.K., Huang, J.C., et al., 2013. A super Asian dust storm over the East and South China Seas: disproportionate dust deposition. J. Geophys. Res.: Atmos. 118 (13), 7169–7181.

Kennedy, M.J., Chadwick, O.A., Vitousek, P.M., Derry, L.A., Hendricks, D.M., 1998. Changing sources of base cations during ecosystem development, Hawaiian Islands. Geology 26 (11), 1015–1018.

Lawrence, C.R., Neff, J.C., 2009. The contemporary physical and chemical flux of aeolian dust: a synthesis of direct measurements of dust deposition. Chem. Geol. 267 (1–2), 46–63.

Li, J.W., Han, Z.W., Zhang, R.J., 2011. Model study of atmospheric particulates during dust storm period in March 2010 over East Asia. Atmos. Environ. 45 (24), 3954–3964.

Li, J., Wang, Z., Zhuang, G., Luo, G., Sun, Y., Wang, Q., 2012. Mixing of Asian mineral dust with anthropogenic pollutants over East Asia: a model case study of a super-duststorm in March 2010. Atmos. Chem. Phys. 12 (16), 7591–7607.

Lin, J.J., Noll, K.E., Holsen, T.M., 1994. Dry deposition velocities as a function of particle size in the ambient atmosphere. Aerosol Sci. Technol. 20 (3), 239–252.

Ma, Q.X., Liu, Y.C., Liu, C., Ma, J.Z., He, H., 2012. A case study of Asian dust storm particles: chemical composition, reactivity to SO_2 and hygroscopic properties. J. Environ. Sci. 24 (1), 62–71.

Mahowald, N.M., Baker, A.R., Bergametti, G., Brooks, N., Duce, R.A., Jickells, T.D., et al., 2005. Atmospheric global dust cycle and iron inputs to the ocean. Glob. Biogeochem. Cycles 19 (4), GB4025.

Meskhidze, N., Chameides, W.L., Nenes, A., Chen, G., 2003. Iron mobilization in mineral dust: can anthropogenic SO_2 emissions affect ocean productivity? Geophys. Res. Lett. 30 (21), 2085.

Neff, J.C., Ballantyne, A.P., Farmer, G.L., Mahowald, N.M., Conroy, J.L., Landry, C.C., et al., 2008. Increasing eolian dust deposition in the western United States linked to human activity. Nat. Geosci. 1 (3), 189–195.

Okada, K., Kai, K., 2004. Atmospheric mineral particles collected at Qira in the Taklamakan Desert. China. Atmos. Environ. 38 (40), 6927–6935.

Olivarez, A.M., Owen, R.M., Rea, D.K., 1991. Geochemistry of eolian dust in Pacific pelagic sediments: implications for paleoclimatic interpretations. Geochim. Cosmochim. Acta 55 (8), 2147–2158.

Pan, Y.P., Wang, Y.S., 2015. Atmospheric wet and dry deposition of trace elements at 10 sites in Northern China. Atmos. Chem. Phys. 15 (2), 951–972.

Paode, P.D., Sofuoglu, S.C., Sivadechathep, J., Noll, K.E., Holsen, T.M., Keeler, G.J., 1998. Dry deposition fluxes and mass size distributions of Pb, Cu, and Zn measured in southern Lake Michigan during AEOLOS. Environ. Sci. Technol. 32 (11), 1629–1635.

Qi, J.H., Li, P.L., Li, X.G., Feng, L.J., Zhang, M.P., 2006. Estimation of dry deposition fluxes of aerosol particles in the Qingdao area II: dry deposition fluxes of six metal elements. Period. Ocean Univ. China 36 (3), 461–467.

Sakai, T., Zaizen, Y., Nishita, C., Matsuki, A., Mano, Y., Okada, K., 2008. Influence of particle nonsphericity on the size distribution measurement of submicrometer mineral dust by use of optical particle counter. Earozoru Kenkyu 23 (4), 269–277.

Shahin, U., Yi, S.M., Paode, R.D., Holsen, T.M., 2000. Long-term elemental dry deposition fluxes measured around Lake Michigan with an automated dry deposition sampler. Environ. Sci. Technol. 34 (10), 1887–1892.

Sheng, L.F., Geng, M., Wang, Y.X., Gao, H.W., Shi, G.Y., Yu, P., 2003. Effects of dust storms on atmospheric aerosols in Qingdao in spring 2002. Res. Environ. Sci. 16 (5), 11–13.

Shi, Z.B., Shao, L.Y., Jones, T.P., Lu, S.L., 2005. Microscopy and mineralogy of airborne particles collected during severe dust storm episodes in Beijing, China. J. Geophys. Res. Atmos. 110 (D1), D01303.

Shi, J.H., Gao, H.W., Zhang, J., Tan, S.C., Ren, J.L., Liu, C.G., et al., 2012. Examination of causative link between a spring bloom and dry/wet deposition of Asian dust in the Yellow Sea, China. J. Geophys. Res. Atmos. 117 (D17), D17304.

Simonson, R.W., 1995. Airborne dust and its significance to soils. Geoderma 65 (1–2), 1–43.

Soreghan, G.S., 1992. Preservation and paleoclimatic significance of eolian dust in the Ancestral Rocky Mountains province. Geology 20 (12), 1111–1114.

Swap, R., Garstang, M., Greco, S., Talbot, R., Kålberg, P., 1992. Saharan dust in the Amazon Basin. Tellus B 44 (2), 133–149.

Tiessen, H., Hauffe, H.K., Mermut, A.R., 1991. Deposition of Harmattan dust and its influence on base saturation of soils in northern Ghana. Geoderma 49 (3–4), 285–299.

VanCuren, R.A., Cahill, T.A., 2002. Asian aerosols in North America: frequency and concentration of fine dust. J. Geophys. Res. Atmos. 107 (D24), 4804.

Wang, Z.H., Xia, Z.K., 2004. Dust flux and particle size of dustfall of the duststorm on March 20–21, 2002 in Beijing. Quat. Sci. 24 (1), 95–99.

Wang, R.F., Feng, Q., Shang, K.Z., 2014. A severe sand-dust storm over China in the spring of 2010. Arid Land Geogr. 37 (1), 31–44.

Yan, H., Gao, H.W., Yao, X.H., Shi, J.H., Yu, C., 2012. Size-dependent mass and dry deposition fluxes of atmospheric aerosols along dust transport routes. Clim. Environ. Res. 17 (2), 205–214.

Zhang, D.Z., 2008. Effect of sea salt on dust settling to the ocean. Tellus B 60 (4), 641–646.

Zhang, D., Iwasaka, Y., 1999. Nitrate and sulfate in individual Asian dust-storm particles in Beijing, China in spring of 1995 and 1996. Atmos. Environ. 33 (19), 3213–3223.

Zhang, D.Z., Zang, J.Y., Shi, G.Y., Iwasaka, Y., Matsuki, A., Trochkine, D., 2003a. Mixture state of individual Asian dust particles at a coastal site of Qingdao. China. Atmos. Environ. 37 (28), 3895–3901.

Zhang, X.Y., Gong, S.L., Shen, Z.X., Mei, F.M., Xi, X.X., Liu, L.C., et al., 2003b. Characterization of soil dust aerosol in China and its transport and distribution during 2001 ACE-Asia: 1. Network observations. J. Geophys. Res. Atmos. 108 (D9), D94261.

Zhang, R.J., Wang, M.X., Sheng, L.F., Kanai, Y., Ohta, A., 2004. Seasonal characterization of dust days, mass concentration and dry deposition of atmospheric aerosols over Qingdao, China. China Particuol. 2 (5), 196–199.

Zhang, D.Z., Iwasaka, Y., Shi, G.Y., 2005a. Sea salt shifts the range sizes of Asian dust. Eos 86 (50), 523–524.

Zhang, D.Z., Iwasaka, Y., Shi, G.Y., Zang, J.Y., Hu, M., Li, C.Y., 2005b. Separated status of the natural dust plume and polluted air masses in an Asian dust storm event at coastal areas of China. J. Geophys. Res. Atmos. 110 (D6), D06302.

Zhang, S., Heller, F., Jin, C.S., Liu, P., Qin, X.G., Liu, D.S., 2008. Grain size distribution and magnetic characteristics of dust fall in Beijing on April 17, 2006. Quat. Sci. 28 (2), 354–362.